JOURNAL OF GEOPHYSICAL RESEARCH, VOL. 93, NO. B4, PAGES 3480–3496, APRIL 10, 1988

Basement Heating by a Cooling Lava: Paleomagnetic Constraints

HARALDUR AUDUNSSON AND SHAUL LEVI

College of Oceanography, Oregon State University, Corvallis

Paleomagnetism can provide quantitative, empirical data on basement heating by cooling lava flows, thereby constraining theoretical models of heat transport processes. We used paleomagnetism to study heating in a Frenchman Springs (FS) lava by the overlying cooling Roza flow. The flows belong to the Miocene Columbia River Basalt (CRB) group, and they recorded very different primary paleomagnetic directions: FS has normal polarity, and Roza is transitional. The solid base of Roza typically rests on a few meters of the brecciated and vesicular top of FS, which is otherwise solid. Thermal demagnetization of FS specimens was usually successful at separating the overprinting due to Roza from the primary FS direction and for establishing limits on the unblocking temperatures of the overprinting. The unblocking temperatures agree well between sites separated by up to 70 km, irrespective of Roza thickness at the sites, which vary from 35–62 m. In specimens from 0.3 to 1 m below the contact, the overprinting was unblocked in the laboratory between 600 and 300 °C and close to 200 °C at 4-m depth. No overprinting was apparent below 6 m. The influence of longer heating times in the field on the unblocking temperatures was estimated by viscous remanence acquisition at elevated temperatures. The results suggest typical reductions of the unblocking temperatures by a few tens of degrees. Our observations imply much less heating of the basement than predicted by simple conductive thermal models. Accounting for the low conductivity breccia in the contact zone results in a better agreement with the experimental temperature profile, but unrealistically low conductivities are needed to sufficiently reduce the absolute temperature. The observed heating is effectively explained by postulating a wet basement at the time of Roza extrusion, as well as groundwater, to maintain a low-temperature isotherm (~100 °C) a few meters below the contact. The presence of water during the time of Roza extrusion and some other CRB flows has been suggested by field observations.

INTRODUCTION

We conducted a paleomagnetic study to determine basement heating by an overlying, cooling lava flow, each with a distinct primary paleomagnetic direction. Knowledge of basement heating will lead to a better understanding of dominant heat transfer mechanisms and thermal evolution of the cooling lava. These data are necessary to relate paleomagnetic measurements to the time of remanence acquisition, so that thick lava flows with sufficiently protracted cooling histories might be used to study high-resolution geomagnetic fluctuations, including normal secular variation and polarity transitions [*Furlong and Shive*, 1983; *Audunsson and Levi*, 1984; *Nyblade et al.*, 1987].

A lava flow crystallizes and cools both through its upper surface and base, thereby heating the underlying basement. A simple solidification and cooling model, assuming heat transfer by conduction only and with constant thermal conductivity and heat capacity, predicts substantial basement heating of up to 300 °C to a depth of half the thickness of the cooling upper flow, giving a high estimate for the cooling time of the flow and the extent of basement heating.

Structural and textural studies of thick Columbia River Basalt (CRB) flows have led *Long and Wood* [1986] to conclude that extensive flooding or extremely high rainfall are required to explain the multiple intraflow alternations of entablature and colonnade structures, which suggest rapid cooling of parts of the interior of these flows. In contrast, relatively simple thermal models were successful in describing the thermal evolution of Alae lava lake in Hawaii [*Peck et al.*, 1977]. However, the cooling of lavas can be very complex, and simple thermal models may be insufficient to explain their thermal evolution, recently shown by paleomagnetic measurements of thick consecutive lava flows [*Nyblade et al.*, 1987].

When a rock with primary thermal remanent magnetization (TRM) is reheated and allowed to cool in a nonzero magnetic field, the primary TRM may be replaced by a total or partial TRM (PTRM) and a high-temperature viscous remanent magnetization (VRM) parallel to the new secondary field. In cases where physical and chemical changes of the magnetic minerals can be ignored, the proportions of the primary and secondary remanences in the rock are determined principally by heating temperature, spectrum of the blocking temperatures, relative intensities of the external fields, and the time the rock spent at and near the maximum temperature. If the rock is heated above its highest blocking temperature, it will be totally remagnetized, but if the maximum heating temperature is within the blocking spectrum, it will usually be only partially remagnetized.

Néel [1949] showed explicitly that for an assemblage of identical noninteracting single-domain (SD) particles cooling from above their Curie temperature (T_c), the magnetic moments are blocked in a narrow temperature range, the blocking temperature, T_b, determined by composition-dependent magnetic properties, grain volumes and shapes, and the associated magnetic anisotropies. The magnitude of the external field and time spent at elevated temperatures will also influence T_b. Thus, blocking temperatures of a PTRM produced in an external field, H_{ex}, and time interval Δt will be different from the unblocking temperatures, T_{ub}, of that PTRM, determined from laboratory thermal demagnetization

Paper number 7B3015.
0148-0227/88/007B-3015$05.00

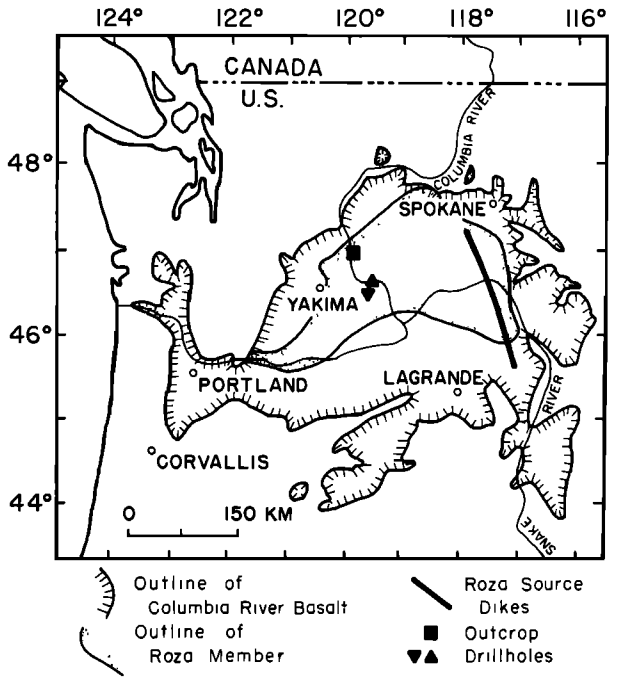

Fig. 1. Location map showing the sampling sites: square, the Frenchman Coulee outcrop; triangles, the drill holes in the Pasco Basin. Exact site locations are given in the appendix. The map was modified after *Swanson et al.* [1975].

with shorter Δt . The Néel derivation shows that for $\Delta t_1 > \Delta t_2$, then $T_{b1} < T_{b2}$. For multidomain (MD) and pseudosingle domain (PSD) grains the blocking process has not been analytically described, but if the underlying physics is similar, analogous relationships might be expected. In general, specimens spend less time at elevated temperatures during laboratory thermal demagnetization experiments than in the field, during production of the original TRM or secondary PTRM. Hence laboratory unblocking of a particular PTRM usually occurs at higher temperatures than its acquisition in nature. The above scenario would be greatly complicated by chemical alteration of the magnetic minerals during heating, which might change the blocking temperature spectrum of the remanence, causing ambiguity in determining T_{ub}, and in cases of extreme chemical alteration, it is possible that no information can be recovered about the heating temperature. Usually, even when the accompanying chemical changes are minor, it is only possible to obtain a range and establish limits on the unblocking temperatures.

To assess the extent to which the cooling Roza flow heated the immediately underlying Frenchman Springs (FS) flow, we sampled the FS as a function of vertical distance below its contact with Roza. Laboratory thermal demagnetizations were used to determine T_{ub}. In addition, VRM acquisition at elevated temperatures was used to empirically assess the overestimation by T_{ub} of the basement heating, caused by differences in heating times.

GEOLOGY

General. The Roza Member of the Columbia River Basalt group has a transitional paleomagnetic direction; it is typically underlain by the normal polarity FS Member, and overlain by the reversed polarity Priest Rapids Member [*Rietman*, 1966]. These units are of middle Miocene age, approximately 15 m.y. The area of the Roza Member was originally over 40,000 km^2 and had a volume of over 1500 km^3 [*Swanson et al.*, 1975]. The source dikes for the Roza are in the eastern Columbia River plateau, and the westerly slope of the region at the time of eruption caused the Roza to flow westward across the Pasco Basin, extending over 300 km west from the source (Figure 1). The Roza Member is usually a single flow in the western region of the plateau, and there are often two flows east of the Pasco Basin [e. g., *Bingham and Walters*, 1965]. Close to its source the Roza may comprise several flows or flow units. *Rietman* [1966] sampled the Roza at nine distant sites and found it to be everywhere transitional with the same characteristic direction. This suggests that the unit was erupted in a relatively short time, probably less than a few hundred years. Where the Roza consists of two or more flows, there is no evidence of interflow sediments or any erosion, and the flow surfaces are commonly intact [*Swanson et al.*, 1975]. Even when flows can be separated based on vesicle zones, they may have cooled as a single unit. It is inferred from emplacement models for the more voluminous flows that they were erupted in few days [*Shaw and Swanson*, 1970].

The underlying FS Member may comprise up to six units [*Beeson et al.*, 1985], and some of these units are comparable to the Roza in extent and thickness. The Squaw Creek sedimentary interbed [*Mackin*, 1961] occurs occasionally in the contact between the FS and Roza members. The Squaw Creek interbed is developed only locally in the west-central plateau, and in the Vantage area the interbed is mostly diatomite, but it grades to siltstone and sandstone as it thickens westward [*Swanson et al.*, 1979].

Sampling Sites. The heating in the FS by the overlying, cooling Roza flow was studied at three sampling sites. An excellent exposure of the Roza/FS contact occurs in Frenchman Coulee, where we sampled the base of Roza and the top 14 m of FS. Similarly in the Pasco Basin the Roza/FS boundary was sampled in two drill cores.

In Frenchman Coulee the Roza is a single 35-m-thick flow, and it was mapped extensively by *Mackin* [1961] and by *Myers* [1973]. The base of Roza appears flat and massive with large columns extending from its base to, commonly, over half the flow's thickness. Higher in the flow, the columns become platy and grade into swirly or fanlike structures, and the top is typically vesicular and blocky. Only a few hundred meters from our sampling site, *Myers* [1973] measured a field section in Roza, where the columns are 4–5 m in diameter, representing about three-fourths of the flow thickness. Based on three vertical sections in the area, *Myers* [1973] observed increased glass content only near the top and in a selvage less than 30-cm-thick near the base of Roza, consistent with the existence of only one Roza flow at this locale. The sampled outcrop at Frenchman Coulee (subsites 40 and 42) has a total lateral extent of about 900 m (see the appendix). A spiracle at subsite 40 might have been produced by steam due to heating of wet sediments or basement groundwater [*Fuller*, 1931]. However, *Mackin* [1961] concluded that Roza spread over predominantly dry surface in this area, based on the absence of pillows at its base and because the underlying sediments may have had mesalike relief of nearly 1 m. In the coulee, the Roza rests on the Sand Hollow flow of the FS Member, whose thickness is slightly less than Roza's. The top few

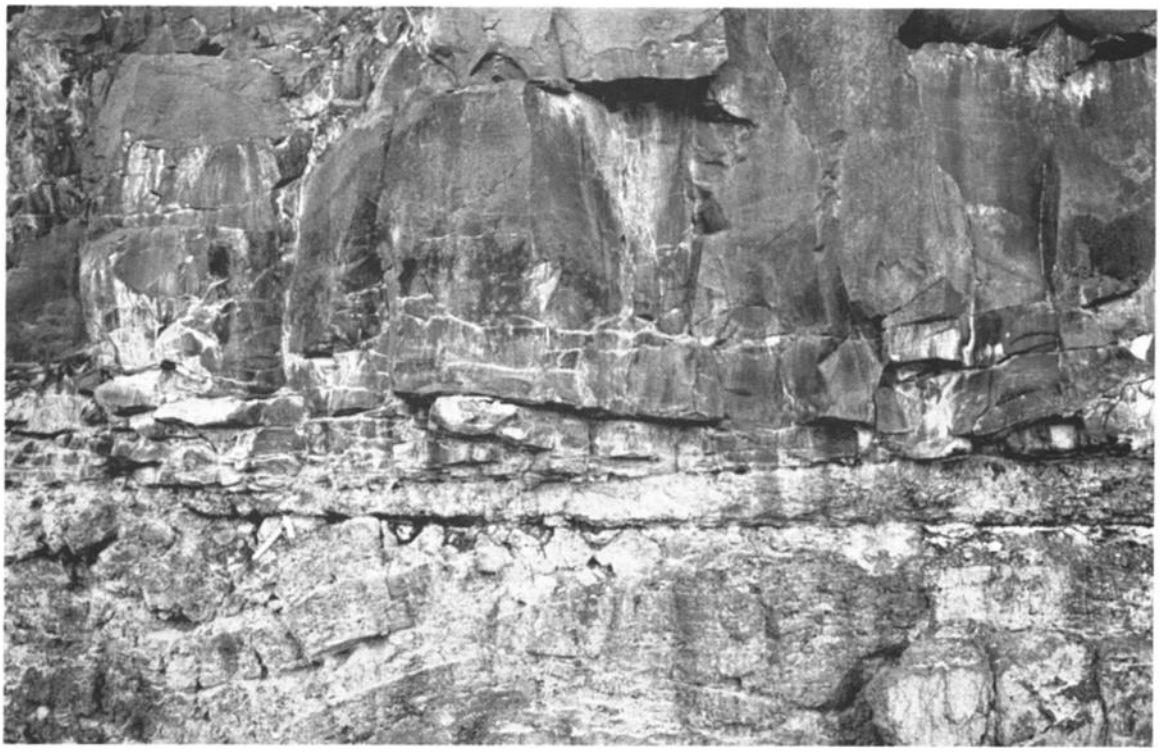

Fig. 2. The Roza/FS contact in Frenchman Coulee at site FS40, showing the sharp contact between the solid Roza resting on the brecciated top of FS (Sand Hollow). The hammer in the lower left corner is about 30 cm long.

meters of Sand Hollow consist of brecciated and vesicular blocks, often with relatively large voids, so the porosity is high (see Figure 2 for typical appearance). Lower, the structure grades into solid, vesicular rock and finally into solid intraflow basalt. Between Roza and Sand Hollow is the Squaw Creek Member, which in the coulee appear as thin, discontinuous sedimentary lenses "consisting chiefly of peaty silt and (or) diatomite" [*Mackin*, 1961, p. 17]. At the sampling sites, the maximum thickness of the Squaw Creek interbed is less than 0.5 m, although it is usually absent.

Subsite 40 is an excellent nearly vertical exposure of the base of Roza and the top 4 m of the Sand Hollow flow, as well as the structure of the Roza/FS contact. At subsite 40 we drilled eight cores from the base of Roza and 20 cores from the Sand Hollow flow over a lateral distance of 300 m. At subsite 42, about 700 m west of subsite 40, we sampled along a dipping surface of approximately 50 m lateral extent. Seven clusters of three to five cores were drilled at different depths in the Sand Hollow, down to 14 m below the contact for a total of 31 cores, including three from the overlying Roza. At subsite 40 the uncertainty in the depth of the cores relative to the Roza/FS boundary is no more than a few decimeters, but it may be as much as a meter at subsite 42. In Frenchman Coulee, samples were drilled using standard paleomagnetic procedures. The cores were oriented with the sun compass while still attached to the outcrop. No correction was made for the bedding attitude, which is only about 1° [*Myers*, 1973].

In the center of the Pasco Basin 60–70 km south of Frenchman Coulee the Roza/FS boundary was sampled in two 63-mm-diameter, azimuthally unoriented drill cores, DC2 and DC12, separated by 11 km (Figure 1). When the Roza extruded, the Pasco Basin was a topographic low, causing Roza to pond in the basin and attain thicknesses of up to 65 m. The Roza occurs as a single flow in the Pasco Basin except in the southeast portion, where two flows or flow units may be present [*Reidel and Fecht*, 1981]. The uppermost FS flow in the basin is the Sentinel Gap [*Beeson et al.*, 1985], with thickness comparable to the Roza flow. The Squaw Creek interbed occurs occasionally in the Pasco Basin drill cores, but it is not present at DC2 and DC12 [*Moak*, 1981]. The contact between the Roza and Sentinel Gap flow in the drill cores appears remarkably similar to that in the Frenchman Coulee outcrop. In both DC2 and DC12 the Roza is a single flow, 62 and 54 m thick, respectively [*Reidel and Fecht*, 1981]. Throughout most of its thickness it is massive, and its base is in sharp contact with the underlying Sentinel Gap flow. The top of Sentinel Gap is vesicular, becoming vesicle free at 3 m below the contact in the sampled drill cores. Horizontal minicores 25 mm in diameter and 63 mm long were drilled from the top 10 m of the Sentinel Gap flow with average spacings of about 0.5 m, sampling 17 and 20 minicores from DC2 and DC12, respectively. For this study we measured 12 and 16 minicores from DC2 and DC12, respectively. Uncertainty in sample depths is of the order of a few decimeters in both drill cores. FS drill core sampling was restricted to the top 10 m below the contact with Roza, because previous paleomagnetic results by *Van Alstine and Gillett* [1981*b*] showed no overprinting due to heating by Roza below about 10 m. The sample distributions with depth at the different sites are shown in Figure 3.

The sampling sites for this research were chosen in areas where geological mapping indicated that the Roza is a single flow. Further evidence that the Roza flow is a single cooling unit at our three sampling sites is provided by the magnetic properties and paleomagnetic directions in drill

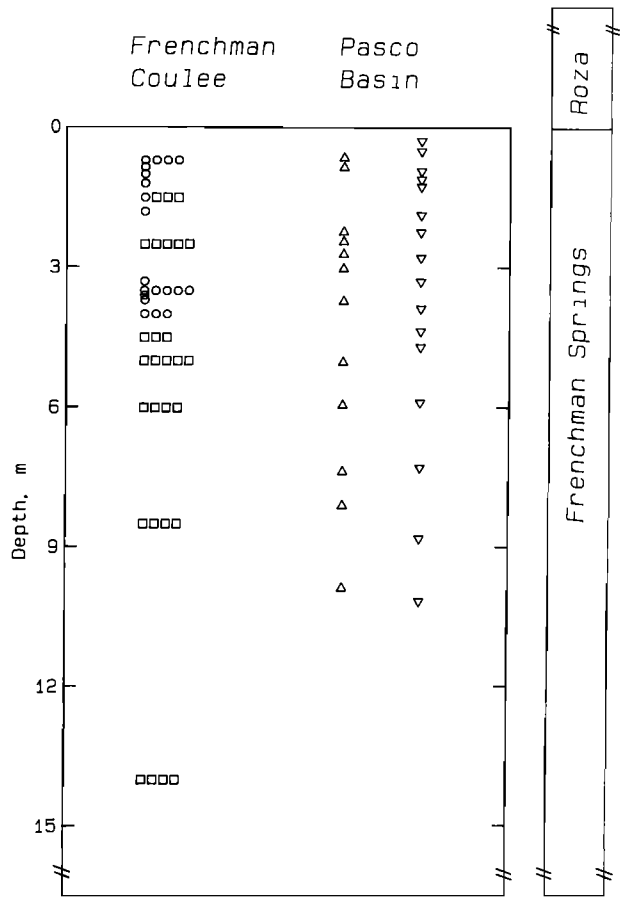

Fig. 3. Samples below the Roza/FS boundary; each symbol represents a distinct core. Circles and squares denote cores from Frenchman Coulee FS40 and FS42, respectively. Triangles and inverted triangles denote cores from the Pasco Basin drill cores DC2 and DC12, respectively. The sampled FS flow is Sand Hollow in Frenchman Coulee, and Sentinel Gap in the Pasco Basin.

cores DC2 and DC12 [*Audunsson and Levi*, 1984] and in an exposed section of Roza approximately 15 km south of Frenchman Coulee (*Audunsson and Levi*, manuscript in preparation, 1987), which is near one of the vertical sections measured by *Myers* [1973] with structure and thickness very similar to the Frenchman Coulee exposure. There are no indications of intraflow quenched zones, which might be expected if the Roza at these sites comprised multiple cooling units. Thus based on macroscopic geological field evidence, petrography, magnetic properties, and paleomagnetic directions, the Roza is a single cooling unit at our sampling sites in Frenchman Coulee and in the Pasco Basin drill cores DC2 and DC12.

THE REFERENCE THERMAL MODEL

To interpret the magnetic results in terms of basement heating by an overlying cooling lava flow, a thermal model is needed. The cooling of lava flows is complex and depends critically on the surroundings, so there may be no single, general thermal model. To provide insight into the cooling process, we first construct a simple model of a solidifying and cooling lava flow which is mostly analytic and incorporates the expected relevant thermal processes. The details may be found in Chapter 11 of *Carslaw and Jaeger* [1959]. This simple model will serve as a limiting reference for comparing the observations. A more complex and realistic model of the cooling history is then constructed using a purely numerical approach constrained by the paleomagnetically determined temperature data.

In the reference model it is assumed that the lava flow was initially a uniform layer of liquid near its melting temperature and in perfect thermal contact with the basement. Solidification and cooling are controlled by heat conduction only. The lava and the basement have the same and constant thermal conductivity and heat capacity. The cooling time which is of interest here is much longer than the time it takes the flow to solidify; therefore one can take advantage of the smoothing properties of temperature diffusion, so variations in initial conditions will be diminished at a later time.

The cooling is divided in two time regimes: first, solidification, followed by cooling via heat diffusion. In nature, lavas solidify over a range of temperatures, but our simple model assumes that the solidification occurs at the initial emplacement temperature. During the solidification phase, the flow is divided in three regions, subdivided by the upward and downward migrating solidification fronts. The top of the flow is kept at a constant ambient temperature, and the solidification front migrates downward into the melt. The molten interior zone is at the melting temperature, and its lower boundary is the lower solidification front migrating upward from the base of the flow. In the crystallized zones, cooling is controlled by simple conduction. The flow is completely solid when the upper and lower solidification fronts merge, signalling the onset of the second time regime, where heat transfer of the entire flow and basement is by simple heat diffusion.

A general way to represent thermal models is to use normalized (dimensionless) variables for depth x and time t. If D and κ denote the flow's thickness and the thermal diffusivity, respectively, the normalized time and depth are

$$\tau = t\kappa / D^2 \qquad \xi = x / D \tag{1}$$

τ, the Fourier number, defines the characteristic cooling time for the flow; ξ, the normalized depth, is 0 at the surface of the flow and 1 at its base. T_0 is the ambient temperature at the surface and the initial temperature of the basement, and T_m is the melting temperature. The normalized temperature T^* is given by

$$T^* = (T - T_0) / (T_m - T_0) \tag{2}$$

such that T^* is initially 1 within the flow and 0 in the basement and on the surface. At the surface, $T^* = 0$ for all τ. Using the normalized variables, only one thermal parameter is needed to compute the general reference model, the Stefan number S,

$$S = (T_m - T_0)C / L \tag{3}$$

where C is heat capacity and L is latent heat of crystallization.

Peck et al. [1977] modelled the cooling of basaltic Alae lava lake, Hawaii. In their final model, to maximize fit with the observations, the thermal conductivity and heat capacity could vary by up to 25% about their mean values in the relevant temperature range. However, constant values for the thermal diffusivity and latent heat gave "good overall agreement with the observed temperatures" [*Peck et al.*, 1977, p. 424]. Hence calculations of simple conductive

TABLE 1. Thermal Parameters

Symbol	Value	Name
T_m	1140 °C	initial (melting) temperature of lava
T_o	10 °C	surface and initial basement temp.
ΔT	100 °C	temperature range of crystallization
C	3×10^6 J/m^3 °C	heat capacity
L	1.1×10^9 J/m^3	latent heat of crystallization
k	1.5 J/s m °C	thermal conductivity
κ	5×10^{-7} m^2/s	thermal diffusivity
S	3.	Stefan number

Values based on *Peck et al.* [1977] and *Murase and McBirney* [1973].

models with constant thermal conductivity and heat capacity are useful as a limiting reference for more realistic models. Assuming that the lava solidifies at a single temperature instead of over a range of temperatures has only a minor effect on cooling, especially at lower temperatures. Typical values of thermal parameters for basalt are given in Table 1; they determine the Stefan number as nearly 3, with a range between 1.5 and 6.

Figure 4*a* shows the temperature distribution in the lava flow and basement for $S = 3$. The flow is completely solid at time $\tau \approx 0.1$ and cools to one-fourth of its initial temperature in time $\tau \approx 0.6$. In Figure 4*b* the maximum heating temperature in the basement is plotted versus depth for different values of S ($S = \infty$ refers to zero latent heat). At the contact between flow and basement the model ($S = 3$) predicts a temperature of 695 °C ($T^* = 0.606$). In the basement the maximum temperature decays nearly exponentially with depth, and the shape of the curves changes slowly with S. This implies substantial basement heating, with temperatures exceeding 300 °C ($T^* = 0.257$) to depth $\xi \approx 1.55$, or just over half the flow's thickness. The variation of basement temperature with time at a given depth is shown in Figure 4*c*; near the contact, the temperature is within 10 °C of its maximum (~2%) for times $\tau \approx 0.1$; that is, 6 and 24 years for cooling flows of 30- and 60-m thickness, respectively.

PALEOMAGNETIC RESULTS

Laboratory Procedures

Each 25-mm-diameter minicore from the outcrop was usually cut in two cylindrical specimens, 15–23 mm in length. From the Pasco Basin drill cores, specimens were taken from the centers of sampled minicores. All remanence measurements were made on a spinner magnetometer. Specimens were demagnetized with a single-axis alternating field (AF) demagnetizer, increasing the AF in steps of 50 to 200 Oe up to a maximum field of 1000 Oe [1 Oe = 1 Gauss = 10^{-4} Tesla]. Thermal demagnetization was done by heating in null field, <10 γ (1 γ = 10^{-5} Gauss = 10^{-9} Tesla), and residual air at diffusion pump pressures of $\leq 10^{-4}$ torr (1 torr = 133 Pa), in steps of about 50 °C up to nearly 600 °C, using smaller steps where the magnetization was expected to change rapidly. Anhysteretic remanent magnetization (ARM) was produced by exposing the specimens to a constant field of 0.50 Oe parallel to an alternating field (400 Hz) decaying smoothly to zero from a maximum of 1000 Oe.

The directional data were analyzed by displaying both the remanent and removed magnetization on stereographs and also by examining vector projection on horizontal and vertical planes. However, in this study we found the stere-

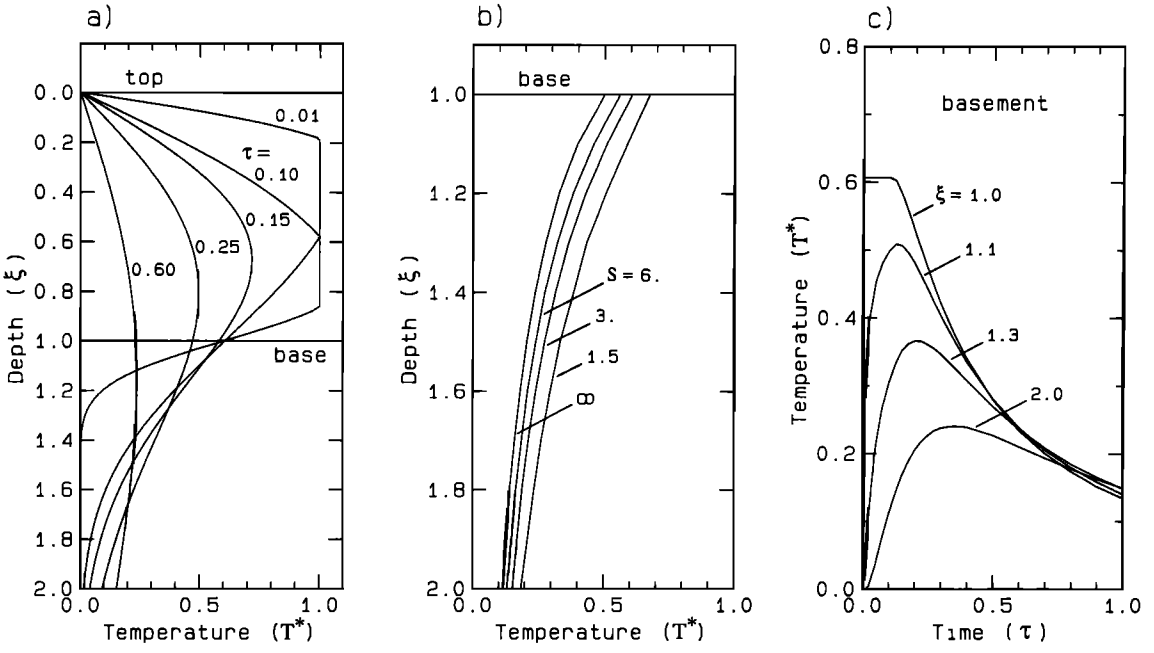

Fig. 4. Temperatures in a cooling lava flow and the underlying basement, using the simple reference thermal model. (*a*) Isochron temperature profiles ($S = 3$); (*b*) maximum basement temperatures for different values of S; (*c*) temperature variations with time at different basement depths below the cooling flow. Temperature, depth, and time are unitless parameters discussed in the text; for a 30-m-thick flow and thermal parameters of Table 1, $\tau = 0.1$ corresponds to 5.7 years.

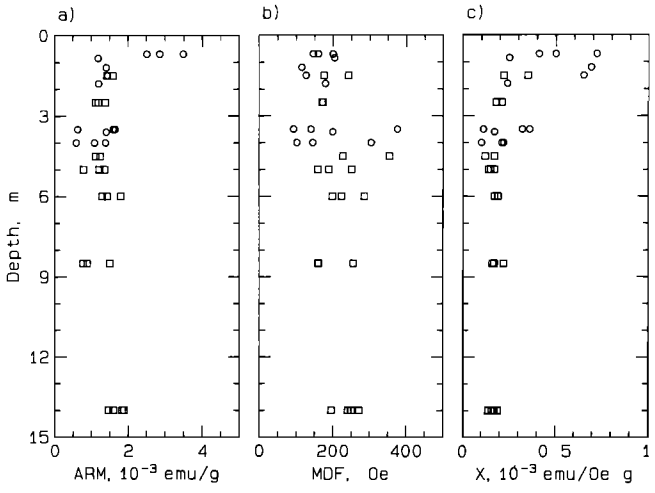

Fig. 5. Variation of magnetic properties with depth for FS specimens from the Frenchman Coulee outcrop. (*a*) ARM intensity (H_{DC} = 0.50 Oe; H_{AF} = 1000 Oe, peak field; H_{AF} parallels H_{DC}). (*b*) ARM stability as measured by MDF, and (*c*) the low field susceptibility. See Figure 3 for explanation of symbols.

ograms to be more illustrative for isolating unblocking temperatures. An upper limit on T_{ub}, designated as $T_{ub,u}$, is the lowest temperature at which only the primary remanence is being removed during thermal demagnetization. The overestimation of $T_{ub,u}$ depends on the extent of chemical alteration and also on the resolution of temperature steps during thermal demagnetization. A lower limit for T_{ub}, $T_{ub,l}$, is the maximum temperature at which only the secondary, overprinting, remanence is removed. The lower limit is difficult to estimate in the presence of modern viscous remanence, which may mask the overprinting caused by low-temperature heating. The best estimate, T_{ub}, is the temperature when the remanence is intermediate between the overprinted and the primary remanence. In this study we determine $T_{ub,l}$, T_{ub}, and $T_{ub,u}$ when possible.

Magnetic Properties

Rietman [1966] reported eight T_c determinations for FS flows, ranging from 220 to 345 °C, and the opaque minerals were identified as titanomagnetite, with no ilmenite lamellae, and ilmenite [*Rietman*, 1966, p. 24]. At least one of Rietman's samples was from the Sentinel Gap flow (Rietman's FS-2) with T_c = 290 °C, and at least one was from the Sand Hollow flow (Rietman's FS-3) with T_c = 255 °C. If the T_c data were obtained for specimens several meters below the flow top, then they are in rough agreement with our thermal demagnetization results, because specimens 2–3 m below the Roza/FS boundary lost at least 80% of their initial remanence by 300 °C.

Heating rocks to high temperatures may cause chemical alteration, modifying their magnetic properties, and such changes might be used to estimate the extent of heating. To delineate the structure near the top of FS and to check for depth-dependent zoning, we examined depth profiles of several magnetic properties.

Figure 5 shows variations of ARM intensity and stability, as measured by the median demagnetizing field (MDF), along with the low field susceptibility for specimens from the Frenchman Coulee outcrop (FS40 and FS42). ARM intensities (Figure 5*a*) are relatively uniform below 1 m from the contact. ARM intensity is doubled for the top three specimens at 0.7 m. ARM stabilities (Figure 5*b*) are uniform below about 5 m, with MDFs between 150 and 300 Oe. Stability is more variable above 5 m. The low field susceptibility (Figure 5*c*) is again uniform below 4 m, but nearer to the contact the values are more scattered and typically higher. The depth variations are different for these three magnetic properties, and no simple zonation can be inferred from these data alone. The most important conclusion from these results is that with respect to these parameters, the FS flow exhibits uniform behavior below about 5 m from contact with Roza.

Thermal demagnetizations of natural remanent magnetization (NRM) and NRM/ARM ratios also provide valuable information about magnetic zoning in the FS flow, suggesting a boundary at about 2 m below the Roza/FS contact. Thermal demagnetization of NRM of specimens below 2 m from the boundary behaved more uniformly, with a narrower range in the median demagnetizing temperatures (MDT) from 150 to 230 °C. (MDT is analogous to MDF of AF demagnetization.) Specimens from within the upper 2 m zone typically had a broader range of MDT between 90 and 540 °C. To compute the ratio NRM/ARM, we used the remanence in the range of alternating fields between 100 and 1000 Oe. The lower level was chosen to reduce the effect of modern VRM in the NRM, and the upper limit is the maximum AF used to demagnetize the NRM and to induce the ARM. Variation of the ratio NRM/ARM with depth is shown in Figure 6. The ratio is quite variable in the 2 m below the contact and has a minimum near 2 m. Between 2 and 5 m the ratio increases systematically. Below 5 m the ratio is essentially constant. Near the flow top the rock is highly inhomogeneous, and the magnetic properties including the NRM/ARM ratios are highly scattered. Because Roza has a transitional direction, its overprinting of FS probably occurred in a considerably weaker magnetic field than the field which pro-

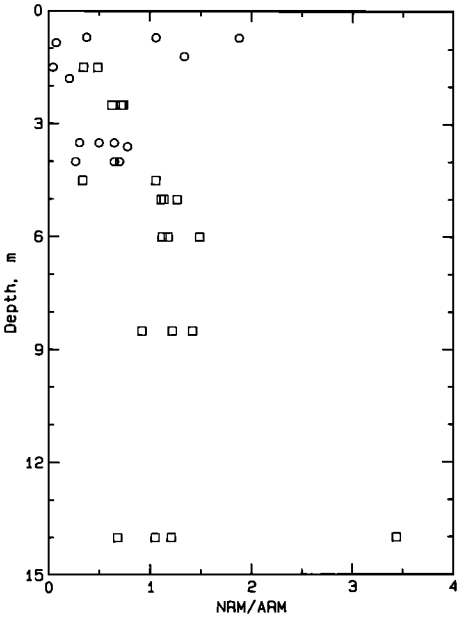

Fig. 6. Depth variation of the ratio NRM/ARM in FS specimens from the Frenchman Coulee outcrop. Symbols explained in Figure 3.

duced the primary FS remanence. Hence the increase in NRM/ARM from 2 to 5 m might reflect a gradual decrease in the overprinting by Roza, which would imply that heating extended no deeper than about 5 m. This agrees well with our conclusions in the next section, based on the unblocking temperatures of the overprinting.

We also measured the magnetic properties of FS specimens from drill cores DC2 and DC12. However, parameters involving NRM, such as NRM/ARM and MDT, were not reliable due to significant overprinting of the drill cores during the original drilling. Variations of the magnetic properties with depth are shown in Figure 7 for specimens from both drill cores. Properties from both drill cores behave similarly with depth except for two specimens from DC2, 0.85 and 2.23 m below the contact, which bracket a missing segment of the drill core, with very low ARM intensities and high MDFs. Specimens from the top 2 m have about twice the ARM intensity and susceptibility as the deeper specimens, excluding the two anomalous specimens. These results are consistent with data from the outcrop in Frenchman Coulee. The most prominent feature of the magnetic properties of the drill cores is increased scatter near the Roza/FS contact, and considerably more uniform behavior beginning 2–3 m below the contact.

The contrasts between upper and deeper specimens may be due to differences in grain size distributions and oxidation states, with smaller grain sizes and more oxidized conditions near the top of the flow. However, it is difficult to ascertain whether these differences are primary or caused by heating due to Roza.

Although magnetic properties have similar variations with depth for the three sites, the absolute values are different. Comparing rock magnetic properties in the deeper, more uniform part of the flow, we find that the drill core specimens are more magnetic, with an average ARM intensity of 2.3 (±0.5) × 10^{-3} emu/g (1 emu/g = Am^2/kg) (the uncertainty corresponds to one standard deviation) and low field susceptibility of 0.43 (±0.18) × 10^{-3} emu/Oe g (1 emu/Oe g = $10^{-3}/4\pi$ m^3/kg), compared with 1.4 (±0.4) × 10^{-3} emu/g and 0.17 (±0.02) × 10^{-3} emu/Oe g in the outcrop, respectively. However, in the drill cores the specimens are less stable, with an average ARM MDF of 100 (± 40) Oe, as compared with 218 (±44) Oe for the outcrop. These data are for 17 specimens from the drill cores, deeper than 2.3 m below the contact, and for 13 specimens from the outcrop, deeper than 5 m from the contact. These differences are consistent with the observation that different FS flows underlie the Roza, the Sand Hollow in Frenchman Coulee, and Sentinel Gap in the Pasco Basin drill cores.

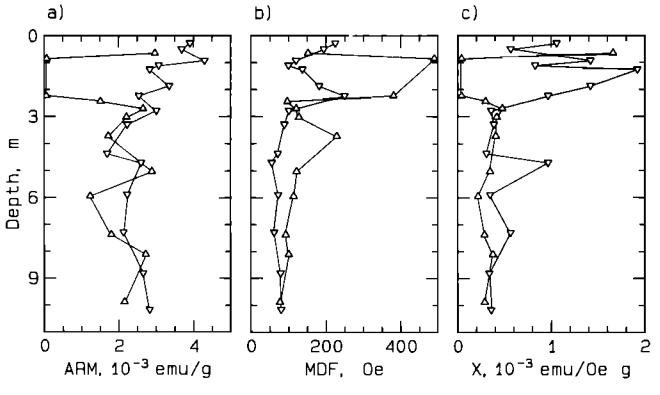

Fig. 7. Variation of magnetic properties with depth in FS specimens from the Pasco Basin drill cores. (*a*) ARM intensity (H_{DC} = 0.50 Oe; H_{AF} = 1000 Oe, peak field; H_{AF} parallels H_{DC}). (*b*) ARM stability as measured by MDF, and (*c*) the low field susceptibility. See Figure 3 for explanation of symbols.

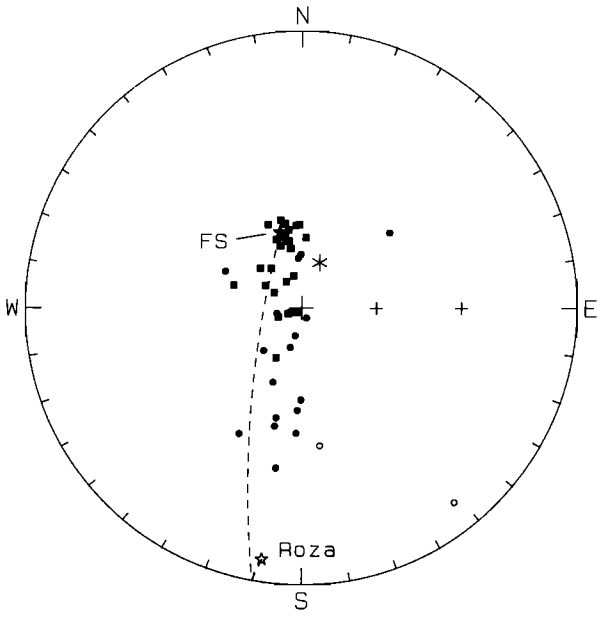

Fig. 8. Stereogram showing the NRM directions of each FS core in the Frenchman Coulee outcrop. Dashed curve is the arc between primary directions of the Roza flow (open star) and the underlying FS Sand Hollow flow (solid star). Solid symbols denote positive inclination (down), and open symbols denote negative inclination (up). Asterisk represents the present field direction. The crosses mark 30° and 60° inclination.

Demagnetization of NRM

Rietman [1966] determined the characteristic remanence direction of the transitional Roza flow at nine widely separated sites, with average values of D (declination) = 189.0°, I (inclination) = −4.8° and α_{95} = 7.0°. Our work on the Roza flow shows nearly identical declinations, but the inclinations vary within the flow from +10° to −5° in the exposures and +5° to −15° in the drill cores, consistent with the Roza's cooling history [*Audunsson and Levi*, 1984, and unpublished data]. At Frenchman Coulee the immediately underlying FS flow (Sand Hollow) has a primary remanence direction D = 344.1° and I = +58.2°, α_{95} = 2.6°. In the Pasco Basin, the underlying FS flow is the Sentinel Gap, and its average stable I = +62.6° with α_{95} = 2.4°. Our values of primary remanence for these FS units are identical to the previous determinations by *Rietman* [1966] (his sites FS-2, 3, and 4), *Van Alstine and Gillett* [1981*a*, *b*] (their outcrop SGA3 and W-4 in DC12), and *Packer and Petty* [1979] (their W-4 in DC2).

Outcrop exposures. Figure 8 shows the NRM directions of all FS cores from Frenchman Coulee. The results are concentrated on an arc between the Roza and FS characteristic directions. The NRMs of nearly all specimens down to about 5 m below the contact show at least some evidence of overprinting, whereas specimens below 6 m show none. The

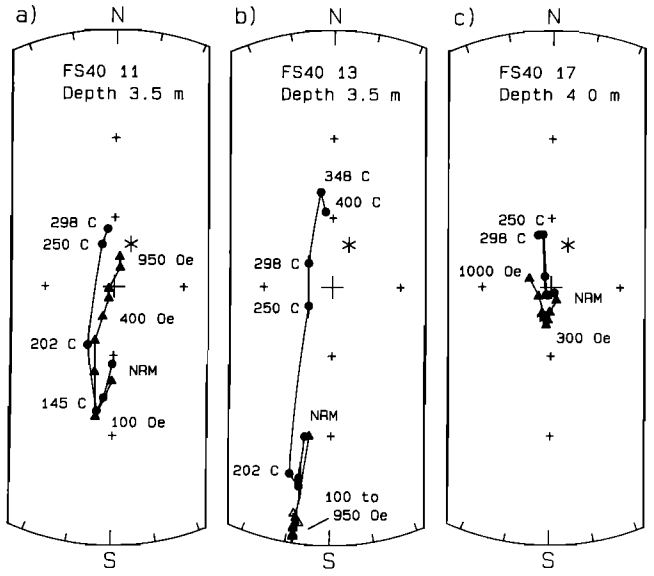

Fig. 9. Comparison of stepwise thermal (circles) and AF (triangles) demagnetizations of NRM of separate specimens from the same core. Symbols as in Figure 8.

slight systematic displacement of most of the NRM directions toward the present field is consistent with a small modern VRM overprint.

AF and thermal demagnetizations of specimens from the same core usually had similar directions. However, some specimens had two remanence components, one with low to moderate T_{ub} and a second component with higher T_{ub}. The higher T_{ub} component could usually be isolated by thermal demagnetization, but it might not be resolvable by AF demagnetization. Comparison of AF and thermal demagnetizations is shown in Figure 9. Figure 9*b* (core FS40 13) is an example of AF demagnetization to 950 Oe, which indicates complete overprinting by the Roza flow, although thermal demagnetization clearly shows only partial resetting. Such differences between thermal and AF demagnetization can occur, because remanence randomized with AF demagnetization usually represents a range of blocking temperatures, and vice versa [*Levi and Merrill*, 1978]. In this study, thermal demagnetization was used to isolate the remanence components acquired in different temperature intervals.

VRM acquired in the recent geomagnetic field is usually present in specimens that have been overprinted by Roza, but it can be removed, together with part of the overprinting due to Roza. Of the nine specimens from the upper 2 m of FS which were thermally demagnetized, six from depths 0.7–1.5 m clearly showed overprinting by Roza. Results from specimen FS40 4 at 1-m depth are shown in Figures 10*a*, and 10*d*; most of the present-day VRM is removed by heating to 100 °C, and the Roza overprinting is nearly completely removed at 300 °C; at higher temperatures the stable remanence is the characteristic FS direction. The remanence behavior during thermal demagnetization of specimens FS40 7 and FS40 8 at 1.2- and 1.5-m depths was not a simple combination of the Roza and FS directions, and although these cores were probably from the same rock piece, they showed quite different remanence directions upon demagnetization. No estimate of T_{ub} could be obtained for these two specimens (Table 2*a*). Specimen FS40 9, at depth 1.5 m, appeared to be completely overprinted, showing only the Roza direction after removal of the VRM, yielding only a lower bound for the unblocking at 550 °C. This value, which is included in Figure 11*a* and Table 2*a*, is rather high when compared with the general trend, and it might be due to complexities of the heating pattern, or, alternatively, the formation of a new high T_{ub} magnetic phase upon heating by Roza. Thus, heating of the Sand Hollow flow in the upper 1.5 m below the Roza/FS contact ranged from over 500 to 300 °C.

Deeper in the flow, from 2.5 to 14 m below the contact, 17 specimens were thermally demagnetized. Ten specimens

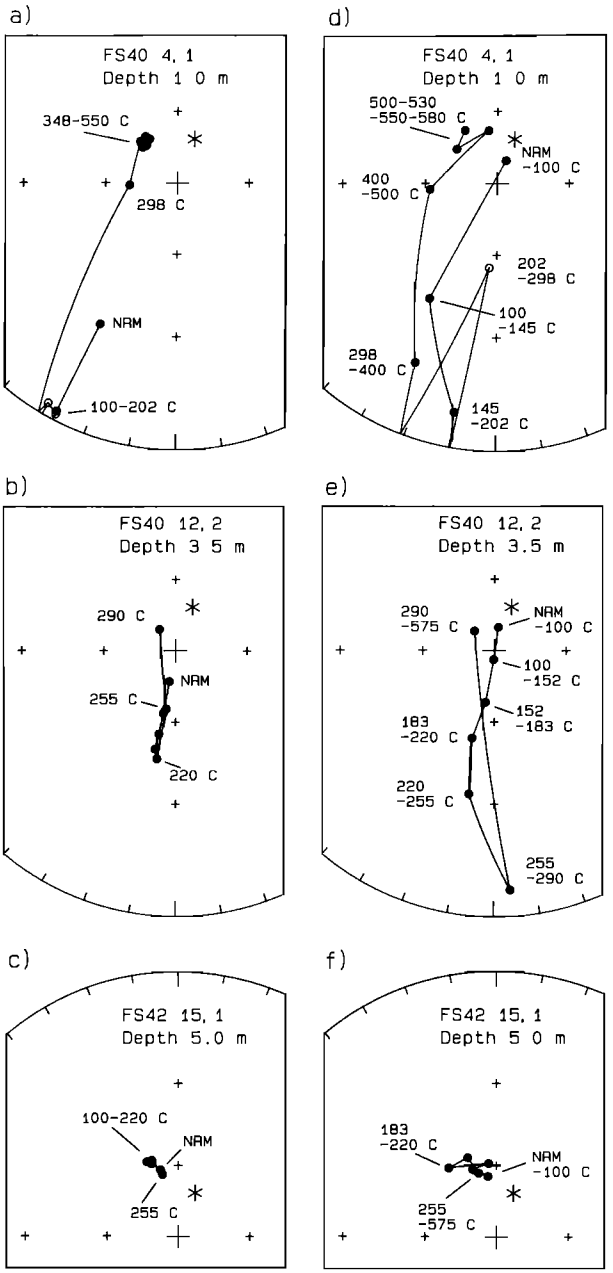

Fig. 10. Examples of thermal demagnetization of specimens from the Frenchman Coulee outcrop; (*a*, *b*) The remanence of partially overprinted specimens. (*c*) Specimen with unaffected remanence. (*d*, *e*, *f*) The corresponding removed remanence. Symbols as in Figure 8.

from depth 2.5–5 m all showed evidence of partial overprinting, removed during progressive thermal demagnetization. Typical behavior for specimens in this depth interval is shown in Figure 9 and Figures 10*b* & 10*e*. The remanence directions trace a loop from the NRM toward the characteristic Roza direction, and in the last few steps stabilize at the primary FS direction. The removed remanence was initially near vertical, suggesting that it was a combination of Roza overprinting and a VRM along the present field. The point on the loop closest to the Roza direction is the best estimate of the overprinting temperature. Although subsites FS40 and FS42 are separated by ~700 m and within FS40 the specimens are distributed laterally over 300 m and about 50 m at FS42, the best estimates for the unblocking temperatures of the Roza overprinting have a narrow range from 200 to 300 °C for specimens between 2.5- and 5.0-m depth. No Roza overprinting was detected in specimens deeper than 5 m below the Roza/FS boundary, and they had stable FS remanence. This suggests an upper limit of about 100 °C for the unblocking temperature of Roza overprinting. The data of one of the shallowest unaffected specimens at 5 m below the contact, FS42 15, are shown in Figures 10*c* & 10*f*. Specimens unaffected by heating were used to obtain the characteristic remanence of FS Sand Hollow flow: D = 344.1°, I = +58.2°, and α_{95} = 2.6°, for N = 12 cores (structurally uncorrected).

TABLE 2. Estimates of Unblocking Temperatures

Specimen		Depth	$T_{ub,l}$	T_{ub}	$T_{ub,u}$
		a. Outcrop, FS40 and FS42			
40	1,2	0.7	550		>579
40	3,2	0.7	500	532	>579
40	4,1	1.0	250	298	348
40	6,2	0.75	338		>338
40	7,1	1.2			
40	8,1	1.5			
40	9,2	1.5	550		
42	1,2	1.5	338	389	550
42	2,1	1.5	338	338	550
42	4,2	2.5		220	255
42	5,1	2.5	183	220	255
40	11,2	3.5	202	250	250
40	12,2	3.5	255	290	290
40	13,1	3.5	202	250	298
40	20,2	3.7	202	250	
40	17,2	4.0	202	202	250
42	10,1	4.5	183	220	220
42	11,2	4.5	183	220	220
42	15,1	5.0			100
42	16,2	5.0	152	183	220
42	18,2	6.0			100
42	19,2	6.0			100
42	21,2	8.5			100
42	23,1	8.5			100
42	27,2	14.0			100
42	28,2	14.0			100
		b. Drill Core DC2			
		0.64			
		0.85	299		>578
		2.23			488
		2.44	201		
		2.71	183	220	220
		3.72	201	251	251
		5.03	100	183	220
		5.95			151
		7.38			100
		8.11			100
		9.88			100
		c. Drill Core DC12			
		0.21	488		
		0.49			
		1.10	532		
		1.86	338	389	>550
		2.23	351	403	>578
		2.78	290		
		3.29	251	299	
		4.36			351
		4.70			220
		5.89			100
		7.29			201
		8.81			201
		10.16			201

Temperature is in degrees Celsius, and depth in meters.

Figure 11*a* and Table 2*a* show the estimated unblocking temperatures versus depth due to Roza overprinting for the FS Sand Hollow flow at the Frenchman Coulee exposure. There is good agreement in the estimates between subsites 40 and 42 for overlapping depths, indicating that the observed heating patterns were similar on a scale of the order of 1 km. There are many possible reasons for the variations in estimated unblocking temperatures for specimens near the contact, including local variations in temperature gradients, differences in primary chemical composition and grain sizes of the magnetic minerals, nonuniformity of secondary chemical changes which would add uncertainty to the estimated unblocking temperature, as well as fluctuations in the heat transfer mechanism.

Drill Core DC2. In DC2, the NRM inclinations in the top 2.5 m were highly scattered, varying between –50° and +66°, but deeper they were between +49° and +80°. The NRM intensities were usually between 1 and 2 x 10^{-3} emu/g, except for two very low intensity specimens at 0.85- and 2.23-m depths (0.02 and 0.04 x 10^{-3} emu/g). Specimens from 11 minicores were AF and thermally demagnetized, and both demagnetizations usually showed similar behavior, as observed for the outcrop samples.

Estimates of the unblocking temperatures are listed in Table 2*b*. The uppermost specimen from DC2, 0.64 m below the Roza/FS contact, had a stable I = –60° and MDT of 450 °C. This sample might have rotated after heating by Roza, and little could be inferred from its unblocking temperature. The specimens at 0.85- and 2.23-m depths had very low intensities and high MDTs. Figures 12*a* & 12*d* show results of the specimen at 2.23 m. The NRM and the thermally demagnetized remanence directions show steep inclinations which stabilize near +65°, similar to the primary FS inclination. This specimen appears to have retained most of its primary remanence, resulting in an upper temperature limit for the heating of 488 °C. The specimen at 0.85 m appears to have been heated to over 299 °C.

The four specimens from 2.44- to 5.03-m depth were at least partially remagnetized. The specimen at 2.44 m had a typical NRM intensity and a low inclination ($I \approx -4$) which survived to 201 °C. Because the remanence is lost at 250 °C, 201 °C is the lower limit on the unblocking temperature of the overprinting. The specimens from 2.71, 3.72, and 5.03

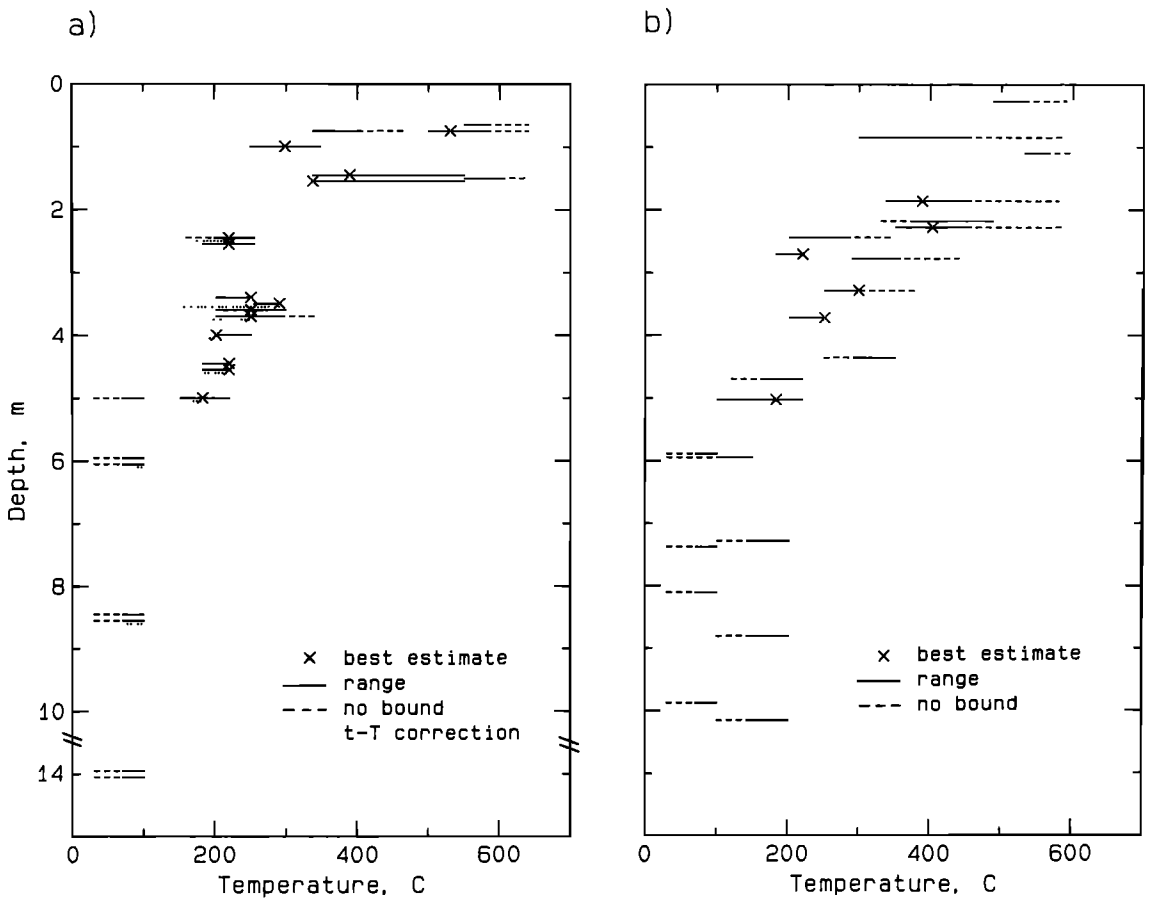

Fig. 11. Unblocking temperatures of the overprinting in FS due to Roza heating. Each bar denotes data from one specimen. (*a*) The Frenchman Coulee outcrop (FS40 and FS42) and (*b*) the Pasco Basin drill cores (DC2 and DC12).

m had been partially overprinted, and Figures 12*b* & 12*e* show the behavior of the specimen at depth 5.03 m. Upon thermal demagnetization, inclinations of the specimens at 2.71 and 5.03 m progressed through near vertical and stabilized at $I = +65°$ at about 220 °C. The initial removed remanences had low inclinations and opposite declinations to the primary remanence (Figure 12*e*), giving a good estimate of unblocking between 180 °C and 220 °C. The third specimen at 3.72 m was not as regular, but it had a horizontal component which was completely unblocked at 251 °C, after which the remanence stabilized at $I = +58°$; hence the best estimate of the unblocking temperature is similar to the other two.

The shallowest unaffected specimen with no significant Roza overprinting was from a depth of 5.95 m, shown in Figures 12*c* & 12*f*, and there is no Roza overprinting for deeper specimens in DC2. The steep inclination of the initial removed remanence may be due to drilling-induced remanent magnetization (DIRM). A soft horizontal magnetization was often present in the deeper specimens, probably a VRM acquired during storage, and it was usually removed in the first heating to 100 °C (Figure 12*f*), which serves also as the upper limit for Roza heating.

Drill Core DC12. The NRM intensites of specimens from DC12 were generally higher and more variable than in DC2, typically of the order of 5 x 10^{-3} emu/g. The NRM inclinations generally steepen with increasing depth, from –33° to +47° in the top 3.5 m, to between +69° and +89° deeper in the flow. The higher NRM intensities and steep inclinations suggest relatively greater overprinting by DIRM in DC12 than DC2. These data are consistent with the relatively lower ARM MDFs of DC12 (Figure 7*b*).

Specimens from 13 minicores were AF and thermally demagnetized, and estimates of the blocking temperatures are listed in Table 2*c*. The top three specimens, at depths 0.21, 0.49, and 1.10 m, showed complex behavior upon demagnetization. The specimens at 0.21 and 1.10 m had intermediate to low inclinations and did not achieve the characteristic FS inclination at higher temperatures; hence only lower limits on the overprinting temperature could be determined. The specimen at 0.49 m had only negative inclination with erratic trends, so it could not be used to determine the unblocking temperature.

The specimens at 1.86- and 2.23-m depth were partially overprinted. Results for the latter specimen are shown in Figure 13*a*, where the remanence exhibits intermediate inclinations, and the directions of removed remanence trace an arc from shallow to steep inclination, giving a best estimate for unblocking near 400 °C. The specimens at 2.78 and 3.29 m below the Roza/FS boundary had shallow initial inclinations that were unblocked at, or just above, 250 °C to 300 °C, after which the directions were scattered (Figure 13*b*). Unfortunately this interpretation for the deeper three specimens at 2.23, 2.78 and 3.29 m is uncertain because the remanences did not stabilize with a declination opposite to

the shallow removed remanence (note that the drill cores were not oriented azimuthally).

The lowest six specimens in DC12, from 4.36 to 10.16 m, were without apparent overprinting due to Roza. The remanence was initially steep, but so was the initial removed remanence. Hence, more likely it was DIRM than overprinting due to Roza. The specimen at depth 7.29 m exemplifies this in Figure 13*c*. The steep overprinting was completely removed by thermal demagnetization of 100–250 °C or 100–200 Oe with AF demagnetization. Thus low temperature and low intensity partial remagnetization due to Roza might have been completely masked by the DIRM and impossible to detect.

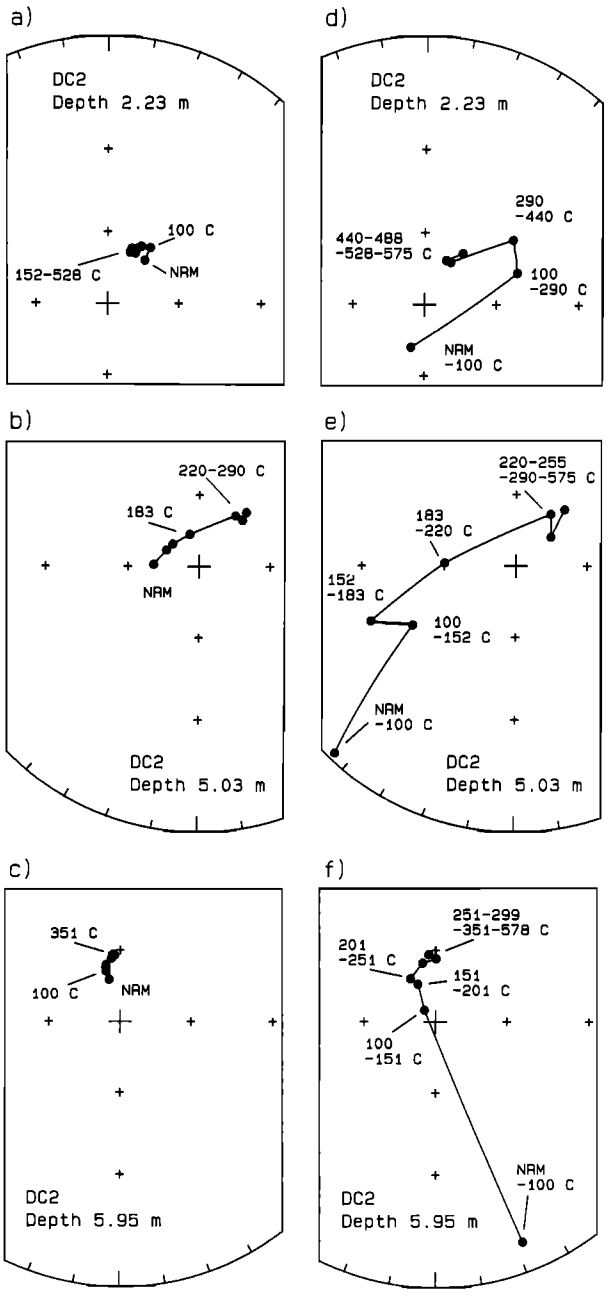

Fig. 12. Thermal demagnetization of specimens from drill core DC2; specimens are from the (*a*) upper, (*b*) intermediate, and (*c*) unaffected group. (*d*, *e*, *f*) The corresponding removed remanence. The declination is arbitrary. Symbols as in Figure 8.

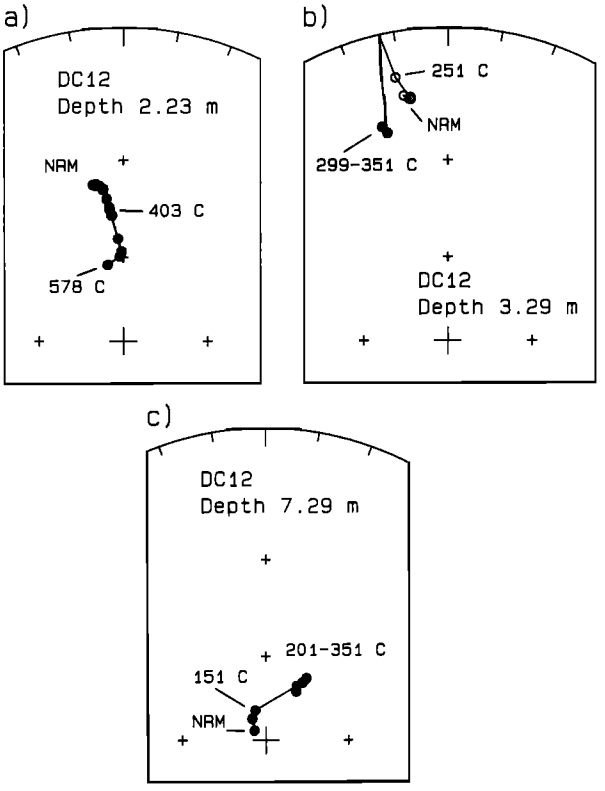

Fig. 13. Thermal demagnetization of specimens from drill core DC12; specimens are from the (*a*) upper, (*b*) intermediate, and (*c*) unaffected group. The declination is arbitrary. Symbols as in Figure 8.

Figure 11*b* gives the unblocking temperature versus depth for DC2 and DC12. Due to the large secondary DIRM in specimens from DC12, they have higher upper bounds on the lower unblocking temperatures than specimens from DC2 and from the outcrop. The two drill core profiles are similar and show no systematic differences, indicating that similar conditions existed at both sites when the Roza flow was emplaced, even though the sites are separated by 11 km.

Specimens from the drill cores, 6–10 m below the Roza/FS boundary and unaffected by the heating due to Roza, have a stable primary remanence direction of $I = +61.9°$, $\alpha_{95} = 4.8°$, $N = 4$ minicores, and $I = +63.3°$, $\alpha_{95} = 2.4°$, $N = 4$ minicores in DC2 and DC12, respectively (structurally uncorrected). The combined data have $I = +62.6°$ with $\alpha_{95} = 2.4°$ and $N = 8$.

Heating Time Effect on the Unblocking Temperature

The unblocking temperatures obtained in the previous section were determined from relatively short laboratory heatings, therefore they represent overestimates of temperatures the rock experienced in the field. In our samples, the domain structure of the magnetic grains varies from MD to SD, as suggested by the MDFs of induced ARMs [*Levi and Merrill*, 1976], and at present there is no satisfactory theory for the time-temperature relationship for remanence of PSD and MD particles. In this section we undertake an approximate, empirical approach to estimate the temperature correction (ΔT_t) due to the effects of longer heating times in the field in lowering the unblocking temperatures.

Remanence unblocking in the laboratory, M_{ub}, occurs during relatively short time t_0, at temperature T_L and in zero

TABLE 3. Viscous Remanent Magnetization

Specimen	Depth	State	S_{25}	S_{100}	$\Delta S/\Delta T$	$\Delta\chi$	VRM/NRM	T_{ub}	ΔT_t
	m		μemu/g Oe		μemu/g Oe °C			°C	°C
40 3,1	0.7	AF	12. (3)	123.(53)	1.5	6	0.08	532	280
40 6,1	0.75	NRM	3.2(1.6)	63.(10)	0.80	1	0.28	>338	125
40 4,2	1.0	NRM	5.7(2.7)	71.(26)	0.87	3	nd	298	nd
42 3,2	1.5	AF	42. (1)	115.(38)	0.98	1	0.18	389	170
42 4,1	2.5	AF	40. (2)	61.(15)	0.28	6	0.05	220	25
40 12,1	3.5	NRM	28. (11)	365.(33)	4.5	18	0.41	290	135
40 20,1	3.7	NRM	77. (18)	178.(61)	1.4	20	0.13	250	55
40 17,1	4.0	AF	39. (2)	64.(19)	0.33	6	0.06	202	20
42 11,1	4.5	NRM	22. (14)	90.(48)	0.91	5	0.07	220	35
42 16,1	5.0	NRM	33. (13)	74.(47)	0.54	18	0.04	183	15
42 19,1	6.0	NRM	8.3(21)	216.(93)	2.8	10	0.03	<100	20
42 23,2	8.5	NRM	47. (28)	263.(92)	2.9	12	0.04	<100	30

S is defined by $M_{VRM} = M_0 + HS \log(\text{time})$. S_{25} and S_{100} are the viscosity coefficients at 25 and 100 °C, respectively, standard deviation is in parentheses (at 25 °C, $N = 6$ points and at 100 °C, $N = 5$ points); $\Delta S/\Delta T$ is the linear increase of S with temperature; $\Delta\chi$ is percent increase of the susceptibility by heating; ΔT_t is estimated lowering of temperature due to longer heating times (equation 10, $t_0 = 20$ min. and $t_T = 20$ years); and VRM/NRM is calculated at $T_b = T_{ub} - \Delta T_t$.

magnetic field. In nature, with longer exposure to heating, this same remanence may have been blocked at a lower temperature, T_F, in a nonzero magnetic field. Following *Briden* [1965], we consider this remanence to have been produced by a two-stage process: first, remanence blocking at temperature $T_F < T_L$ and time t_0, comparable to the unblocking time in the laboratory, and, second, VRM acquired during time t_F and temperature T_F. The total magnetization is then the sum of these two:

$$M(T_F, t_F) = \text{PTRM}(T_F, t_0) + \text{VRM}(T_F, t_F) \quad (4)$$

and

$$M_{ub}(T_L, t_0) = M(T_F, t_F), \quad T_L > T_F, \quad t_0 < t_F \quad (5)$$

where it is assumed that M_{ub} and M were produced in the same external field. PTRM (T_F, t_0) is estimated from the laboratory thermal demagnetization curves at T_F, assuming that there is no field dependence of the blocking temperatures for geomagnetic field intensities. VRM can often be described by the empirical isothermal equation

$$\text{VRM}(T, t) = M_0 + HS(T) \log(t) \quad (6)$$

where S is the viscous remanence acquisition coefficient determined from VRM acquisition experiments, H is the external field and M_0 is constant. Given the laboratory thermal demagnetization curve and (6), then for a particular T_L and H, t_F and T_F can be determined iteratively.

VRM production varies with temperature. Therefore one must consider its acquisition as the temperature approaches and then slowly decreases from its maximum heating temperature. Thermal modelling shows that the temperature increase is much faster than the cooling (of the order of 5 times; see, for example, Figure 4*c*). In addition, for the ascending limb of the temperature profile, VRM is recorded only in remanence with blocking temperatures $\geq T_p$, where T_p is the peak heating temperature. During cooling, VRM is produced in all accessible blocking temperature regions. For these reasons, only the cooling limb is considered in our approximate calculation for VRM production. Based on computed thermal models, a reasonable approximation for the decrease of temperature with time is

$$T(t) = T_p / (1 + t/t_T) \quad (7)$$

where t_T is the decay time, such that the temperature is halved for $t = t_T$. The viscosity coefficient is assumed to depend linearly on temperature,

$$S(T) = S_0 + aT \quad (8)$$

where S_0 and a are constants. Using (7) and (8) the VRM acquisition can be written explicitly by integrating

$$dM = HS[T(t)]\, d\log(t) \quad (9)$$

This shows that the VRM acquisition can be decomposed in two parts; one is isothermal and the other depends on cooling rate. An equivalent result can be derived from this by assuming that the VRM is acquired entirely at the maximum temperature (T_p) for some effective time, t_e. For $S_0 \ll aT_p$ the effective time is shown to approximately equal the decay time, $t_T \approx t_e$, and the VRM acquisition can therefore be written as

$$\text{VRM}(t) - M_0 \approx HS(T_p) \log(t_T / t_0) \quad (10)$$

where it is assumed $t_0 \ll t_T$.

To determine the viscous remanence acquisition coefficient, $S(T)$, and to estimate its temperature dependence, VRM was produced in specimens from the outcrop (FS40 and FS42) at room temperature and at 100 °C; each experiment lasted 1 week (10^4 min). Heatings were conducted in air and an external field of 0.42 Oe; the VRM was measured at room temperature. Eight specimens had NRM, and four had been previously AF demagnetized to 1000 Oe. Using specimens with NRM as the initial state for the VRM experiments caused larger measurement errors in the acquired VRM than for initially AF demagnetized specimens; however, the NRM condition is closer to the state of the rock during heating by Roza. The VRM increased linearly with log (t) for times 10^2 to at least 10^4 min. Computed values of the viscosity coefficient are given in Table 3, and the VRM acquisition of five specimens is shown in Figure 14. To monitor magnetic changes in the rock during heatings at 100 °C, we measured the low field susceptibility before and after the heatings. In all specimens the susceptibility increased by 1–20% (Table

3). We believe that the largest effect on increasing the susceptibilities is annealing relaxation of the magnetic material [*Cullity*, 1972; pp. 320 & 353], rather than chemical alterations. The ARM acquisition and stability of the four AF demagnetized specimens were determined before and after the heatings. Three specimens showed only small changes, ≤5% in MDFs and ≤2% in intensity. However, for one specimen (FS40 17) the MDF increased 14% and the intensity decreased 6%.

In the thermal demagnetization experiments the time the specimens spent at elevated temperatures, within 10 °C of maximum, was of the order of a few tens of minutes. In contrast, the simple thermal model predicts the corresponding time to be 6 and 24 years ($\Delta\tau \approx 0.1$) near the base ($\xi = 1.1$) of 30- and 60-m-thick flows, respectively, and the decay times (t_T) approximately 25 and 100 years ($\Delta\tau \approx 0.4$) (Figure 4*c*). A more realistic model, which includes hydrothermal effects, will be discussed in the next section; it predicts comparable cooling times, although the maximum attained temperatures are lower.

To estimate the VRM component in FS due to overprinting by Roza, field strength and duration of heating are required. The overprinting occurred during a geomagnetic reversal, which would suggest a reduced paleointensity. We arbitrarily set the field strength at 0.1 Oe (our preliminary paleointensity experiments of Roza were not successful). The decay time is not well constrained, and in the outcrop the thermal models suggest that it is about 20 years; hence t_e = 20 years, and t_0 is approximately 20 min. The VRMs were calculated from (10), and the temperature correction (ΔT_t).was determined by iterations. To assess the uncertainty in ΔT_t we evaluated the correction for different times, field strengths, and unblocking temperatures. Changing the time from 1 to 100 years altered ΔT_t by less than 20%. However, varying the field strength from 0.05 to 0.2 Oe or modifying the unblocking temperature by ±50 °C caused significant changes in the calculated ΔT_t values, averaging about 50%. The best estimates of the temperature corrections (ΔT_t) are given in Table 3 and in Figure 11*a*.

The correction to the unblocking temperature is of the order of tens of degrees. Specifically, in the depth range 2.5–8.5 m, temperature reductions range from 15 to 135 °C. For specimens within 2.5 m from the contact, temperature corrections vary from 125 to 280 °C. However, near the Roza/FS contact, our results are less valid because of uncertainties in extrapolating S beyond 100 °C. Moreover, chemical alterations which have been neglected are more likely to occur at higher temperatures.

The estimated heating temperatures are slightly lower than the unblocking temperatures, but the differences are small and have only a minor effect on the overall temperature heating profile (Figure 11), especially in comparison with the uncertainties in T_{ub}. Therefore in this study laboratory-determined unblocking temperatures serve as a reasonable approximation to actual heating in the field.

Summary of Paleomagnetic Results

Paleomagnetically determined temperature profiles indicate that the cooling Roza flow produced very similar heating in the underlying FS lavas at Frenchman Coulee and the Pasco Basin drill cores. This is surprising in the context of the simple conductive thermal model, because in the Pasco Basin the Roza is nearly twice as thick as in Frenchman Coulee (54–62 m versus 35 m). In both areas, heating to above 500 °C was restricted to within 2 m below the Roza/FS contact. In this zone, heating may also have been accompanied by chemical alteration of magnetic minerals; however, even in the upper 2 m most of the specimens were not completely remagnetized. Between 2.5 and 5 m there was partial remagnetization of the FS flows, but there was no evidence for chemical alteration. Heating probably did not exceed 300 °C at 4-m depth. The data indicate that below 5–6 m from the Roza/FS contact there was no apparent heating at either drill cores or outcrop. The main difference between the outcrop and drill cores is the somewhat greater heating temperatures in the upper 3 m of the drill cores, which is consistent with the greater thickness of Roza in the Pasco Basin. However, below 3 m from the contact, the unblocking temperature profiles in the drill cores and outcrop are similar, approaching 200 °C at 4-m depth. Because the drill cores are azimuthally unoriented and were affected by significant DIRM, their results are less certain than for the outcrop. However, the similarity of the paleomagnetically determined temperature profiles in the FS flows (Figure 11) with different thicknesses and separated by about 70 km is unmistakable, implying that basement heating due to the cooling Roza was considerably less than predicted by the simple conductive thermal model, suggesting that more complex thermal models are necessary to explain the observed heating.

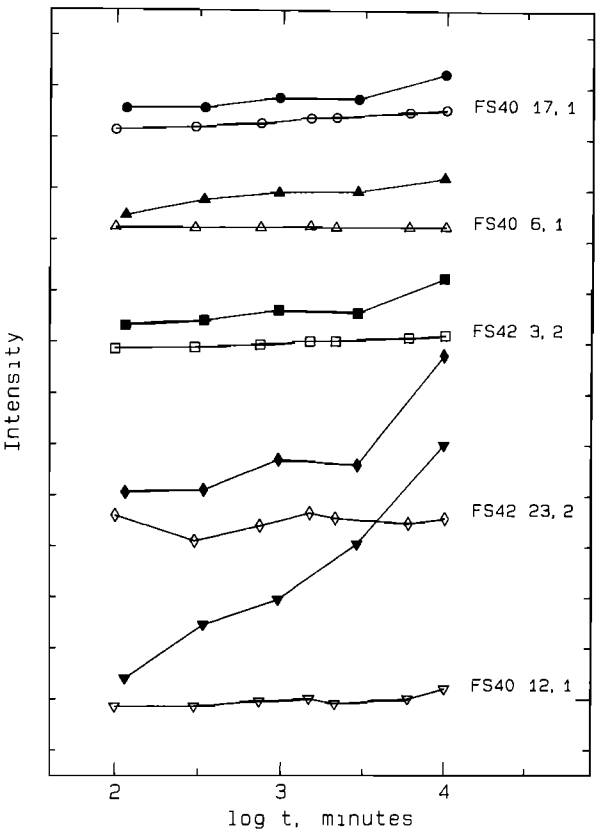

Fig. 14. VRM acquisition of selected specimens at 25 °C (open symbols) and at 100 °C (solid symbols). The ticks on the intensity axis correspond to increments of 2×10^{-3} emu, but the absolute intensity is arbitrary.

THERMAL MODEL CONSTRAINED BY PALEOMAGNETIC OBSERVATIONS

With the possible exception of very near the contact, the basement temperature profile obtained from the paleomagnetic results indicates considerably less heating and to shallower depths than predicted by the simple reference thermal model. One can calculate the thickness of a cooling lava needed to cause the observed heating, assuming the validity of the simple reference thermal model. At 4 m below the contact, maximum heating is approximately 200 °C (Figure 11). This would require a flow which is about 4.5 m thick, placing its top in the lower third of the Roza colonnade, where there is no hint of a flow boundary. Modifications of the reference model therefore appear necessary to explain the observations.

The thermal problem is basically twofold: first, the characteristics of the heat source causing basement heating, the amount and distribution of thermal energy; and second, the thermal characteristics of the basement, the mechanism of heat transfer and the rate of heat absorption. Temperature at the contact between the flow and basement and the length of heating are simultaneously determined by the nature of the heat source and of the basement.

Heat Source Characteristics: Emplacement and Cooling of Lavas

For our discussion it is important to know the initial distribution of thermal energy within the flow, which is predominantly controlled by heat loss during emplacement. For example, a turbulent lava flow has uniform temperature distribution, and the heat is radiated efficiently. As viscosity increases with crystallization and decreasing temperature, turbulence ceases and the flow becomes laminar. The transition to laminar flow may occur within a few days for a 30-m-thick flow, which is short compared with the total cooling time. Therefore, if initially the flow was turbulent, the initial temperature distribution for laminar flow is practically uniform, but possibly with significantly reduced latent heat. During laminar flow, solid crusts form quickly at the surface and base with liquid magma flowing between, and the lava's cooling may be described by the simple reference model. However, the spreading lava might be expected to overturn cool scoria from the top to its base, which will consequently be heated, in effect shifting upward the thermal base of the flow. Using this simple view, we infer, first, that the emplacement temperature is practically uniform, except for an effect due to scoria at the flow's base and top, and second, because neither the basement nor the top crust can distinguish whether the magma is still flowing or if the lava is thickening, the heating in the basement will only reflect the total heating time, controlled by the final thickness of the flow. Thus apparently, the only significant modifications of the cooling lava (heat source) to the simple reference thermal model are (1) reduced latent heat and (2) the possible presence of reworked relatively thin and cold or crusts at the base of the flow. Reduction of the latent heat by half doubles the Stefan number. Increasing the Stefan number from 3 to 6 reduces the maximum basement temperature (Figure 4*b*). Furthermore, due to the averaging properties of temperature diffusion, basement heating is relatively insensitive to small variations in the distribution of thermal energy within the overlying flow.

Basement Characteristics: Processes of Heat Transfer

The observed heating decreases rapidly immediately below the base of the flow, implying a discontinuity in heat transfer parameters near the top of the basement, which may arise from possibly three modifications of the reference model: first, the effects due to the observed highly porous layer at the contact; second, the presence of groundwater; or third, a combination of the two. To evaluate the effects of the above processes on the temperature distribution in the heated flow, we used a numerical method. This permits the thermal conductivity and heat capacity to depend on temperature and depth, adding flexibility to incorporate different cooling mechanisms by modifying these parameters. The equation of heat diffusion is approximated with the implicit finite difference approximation [see, e.g., *Clausing*, 1969]. The release of latent heat is accomplished by increasing heat capacity in the temperature range of solidification [e.g., *Jaeger*, 1967; *Bonacina et al.*, 1973]. We compared our numerical method with several available analytical solutions, with and without latent heat [*Carslaw and Jaeger*, 1959]. For these solutions, maximum deviations were within 1%. In the following thermal models, the thermal parameters, whose values are listed in Table 1, are taken to be temperature independent, except for heat capacity, which is increased in the solidification range (1140–1040 °C) to incorporate latent heat. We always state explicitly whenever the thermal parameters are changed.

The first modification of the reference model accounts for the porous zone at the top of the heated flow, which decreases thermal conductivity and is important in controlling temperature in the basement and within the flow. For example, in a basalt a 20% porosity (air-filled pores) would typically reduce bulk thermal conductivity by 30–50% from the nonporous state [*Robertson and Peck*, 1974]. Also, in porous breccia, often present at the top of lava flows, thermal contact between rock fragments may be poor due to imperfect alignment of touching surfaces and small interstitial grains and can effectively reduce bulk conductivity as compared with solid material. These two effects may therefore profoundly reduce bulk conductivity. In computing the effect of a low-conductivity layer in the contact between the flows, we assumed the heat capacity to be independent of the conductivity and to be half the value of the solid lava. We calculated temperature distributions for several different conductivities, expressed as fractions of the value of the solid rock in adjacent flows. Based on field data and observed heating temperatures, the zone of breccia and high porosity was estimated to be 3 m thick. Figure 15*a* shows the effect of introducing a 3-m low-conductivity layer with different conductivity contrasts. A very high temperature gradient appears near the base of the flow with a linear decrease in temperature, indicating the control of the zone on heat transfer. The lower conductivity layer increases the contact temperature and lowers the temperature at its base. Below the high-gradient region, maximum temperature decreases slowly with depth. Increasing the thickness of the insulating layer is relatively inefficient in lowering temperature near the contact, although the greater thickness will lower the temperature at greater depths. In general, the insulating zone decreases the symmetry of cooling in the overlying flow.

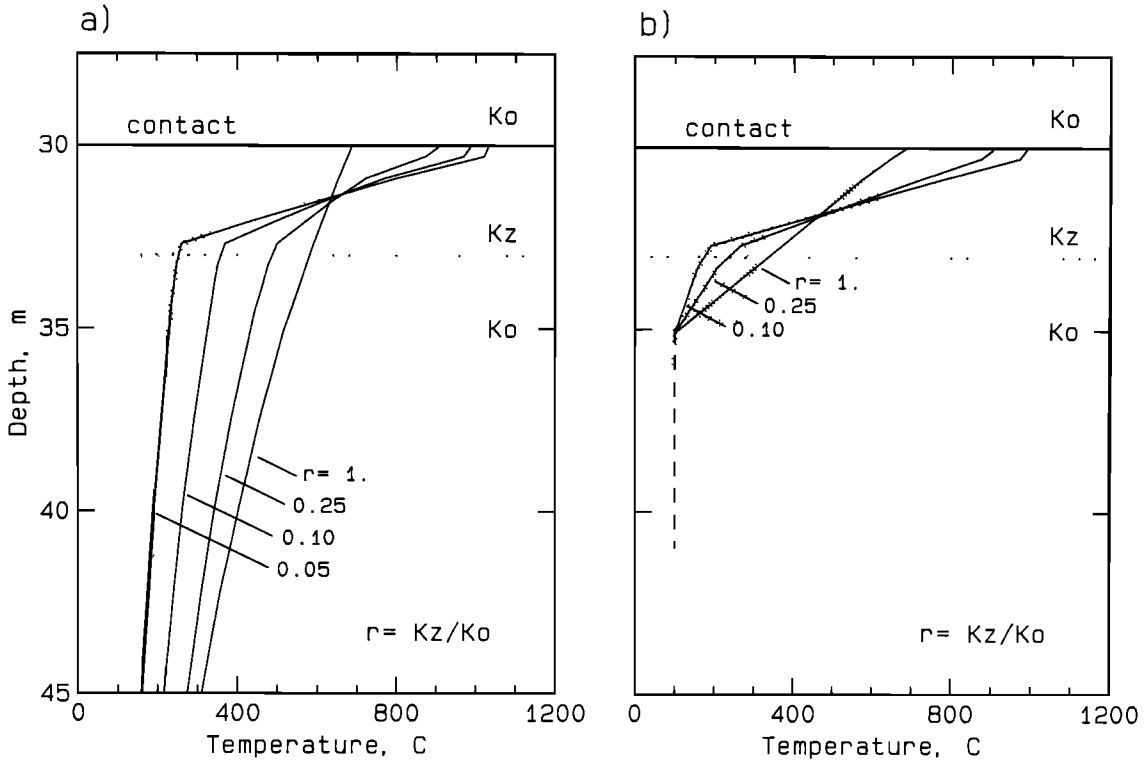

Fig. 15. Calculated maximum basement temperatures below a 30-m-thick cooling lava flow. (*a*) Different low conductivities in a 3-m zone at the top of the basement and (*b*) also assuming a 100 °C isotherm 5 m below the contact. Shaded area represents the observed heating temperatures.

We now consider the effects of groundwater in absorbing heat from the overlying flow. Numerous situations of varying complexity can be envisioned. If the lava spread over wet sediments overlying a dry basement, the net effect of heating and vaporization of water is to rapidly cool the base of the flow, causing the effective, or thermal, base of the flow to move upward. For example, a 1-m layer of water will move the thermal base of the flow by nearly 0.6 m. The effect on basement heating can be approximated by shifting the temperature distribution upward proportional to the amount of water at the base, resulting in lower basement temperatures at given depths. On the other hand, if the basement is wet or the groundwater table is relatively shallow, a complex initial situation is expected, and water advection may possibly occur [*Udell*, 1983]. The extent of advection is affected by the amount of available water and the structure of the underlying flow. If the steady state evolves quickly, the thermal profile can be approximated by assigning a constant temperature, the boiling point of water, at some depth. The present data suggest that a 100 °C isotherm might occur in the vicinity of 5 m below the contact. Figure 15*b* (r = 1) shows the computed maximum basement temperature due to an overlying 30-m-thick flow constrained with a 100 °C isotherm 5 m below its base. Because temperatures at the top of the flow (10 °C) and near its base (100 °C) are similar, cooling is nearly symmetrical. The shallow isotherm does not seriously alter the initial contact temperature, but 3 m below the contact, the maximum temperature is reduced significantly, from nearly 600 °C down to 350 °C. This temperature would increase, of course, for greater depths of the 100 °C isotherm.

The third analysis combines the effects of porosity and groundwater, using a 3-m-thick low-conductivity zone and a 100 °C isotherm at 5-m depth below the flow's contact. The computed profile of maximum basement temperatures is shown in Figure 15*b*, resulting in a better fit to the data than by considering the two factors separately.

Preferred Thermal Model

Geological mapping, rock magnetic and paleomagnetic data indicate that the Roza flow is a single cooling unit at all our sampling sites, and there is no evidence for cooling of the flow's base prior to emplacement. Even if the flow spread in spurts, forming several "units," they must have been hot enough to coalesce and then cool as a single unit, because there are no vesicle or glass zones within the sampled Roza. Emplacement of the voluminous CRB flows was discussed by *Shaw and Swanson* [1970]. They concluded that during spreading, the flows were predominantly turbulent and that they were emplaced during of the order of 1 week. Water-quenched rims of pillows far from Roza's vent area have glass that typically contains only a few percent microlites, showing that minimal cooling took place during emplacement [*Swanson et al.*, 1975]. Furthermore, we concluded in earlier discussions, by considering very simple spreading, that preemplacement cooling has small effect on heating temperatures of the basement, and, were the lava half crystallized at emplacement, the temperature would be lowered by about 50 °C as compared with completely liquid flow. It appears therefore that preemplacement cooling of the Roza flow is an unlikely cause for the limited extent of basement heating, but it cannot be entirely ruled out, due to

limited knowledge about spreading mechanisms. Thermal characteristics of the basement are therefore a more likely source controlling basement heating.

Breccia occur in the boundary between the Roza and FS flows, and the rock is vesicular in the top few meters of the FS flow. This field evidence requires a thermal model with lower conductivity near the contact, which would give rise to a higher temperature gradient in the porous zone, in agreement with paleomagnetic results. However, unrealistically low conductivity, ≤5% of its value in the solid flow and basement, would be required to adjust the thermal model to reproduce the observed heating temperatures (see Figure 15*a*). However, the thermal conductivity of air is ~2% of the conductivity of solid basalt, and convection of air is not expected because heating is from above. Therefore we consider it likely that heat extraction by groundwater had occurred to explain the observed temperature profile. Requiring groundwater to maintain the 100 °C isotherm at 5 m below the Roza/FS contact results in a good fit of the data below 3-m depth, but the predicted temperatures in the low conductivity zone are too high (see Figure 15*b*). In addition, maintaining a sufficient pool of groundwater near the base appears problematic because the underlying flow is mostly solid and therefore unlikely to allow much advection. On the other hand, contacts between lava flows are known to be good conduits of groundwater, and by this mechanism, sufficient water might be supplied to cool the basement. This flow of groundwater may be runoff from distant areas and/or local rainwater that fell on Roza. Hot lava is generally impermeable to water, but sinks may form locally in the hot lava, permitting water to run through and enter the basement.

To constrain possible situations, it is valuable to know the expected heat absorbed by groundwater at the flow's base. When a low-temperature isotherm (~100 °C) is imposed near the base of the lava, the heat flows from the lava's upper surface and its base are nearly equal. If the average temperature within the flow has fallen to ~300 °C in 10 years in a 30-m-thick unit, heat flow through the base is estimated to be nearly 1×10^{10} J/m^2 year. This is an overestimate because cooling is not exactly symmetrical and insulating scoria at the base will reduce heat flow there. Heat at the base is mostly taken up by groundwater and partially by basement rock. Assuming that groundwater takes up half the heat flow above (~5×10^9 J/m^2 year), and if groundwater is only heated by ~50 °C, the equivalent of a 25-m layer of water would be needed every year. However, if the water evaporates completely, heat extraction is much more effective, and only 2 m of water would be required annually. Thus between 2 and a few tens of meters of groundwater are needed each year. In addition, if steam were able to vent through the overlying lava, similar to the mapped spiracle in Roza at Frenchman Coulee, it would be very efficient in removing heat from the basement.

Hodges [1978] studied basaltic ring structures in the Roza flow near Odessa in east central Washington and concluded that when Roza was partially solidified, the groundwater table rose into the flow, causing explosive venting and cracking. Even if this rise of the water table were a local phenomenon, it shows that there was groundwater available at shallow depth when Roza extruded.

It is likely that the ground on which the Roza flowed was intermittently wet, as supported by the presence of the large spiracle, diatomites, and the glassy selvage at its base in Frenchman Coulee. Generally, however, the base of Roza is solid, with wide regular columns several meters across, suggesting extrusion mainly onto dry ground. The immediate cooling due to wet ground at the contact is therefore expected to be small but possibly sufficient for a small upward shift of the thermal boundary of the cooling flow, which would have had a profound effect on reducing temperature in the porous zone at the top of the basement. As previously discussed, a relatively cold flow bottom at the time of emplacement would further aid in moving upward the effective thermal base. Including the low-conductivity zone at the top of the basement improves this model slightly, but the extraction of heat by water still would be the predominant cooling mechanism.

At present, the preferred scenario is that the Roza extruded over a wet surface, thereby shifting upward its thermal base and lowering the maximum temperature near the contact. A low-temperature isotherm was soon established a few meters below the boundary by groundwater, which subsequently controlled the cooling along with the low-conductivity breccia at the top of the underlying flow.

CONCLUSIONS

In this study, paleomagnetic measurements were used to determine the temperature profile in basement rock heated from above by a thick cooling lava flow. Although the cooling lava was up to 60 m thick, there was no evidence that the temperature in the underlying basement exceeded 100 °C at depths greater than 6 m below the contact, which is considerably less than predicted by a simple conductive thermal model. The combined paleomagnetic results and thermal modelling suggest that the thermal history was affected by the presence of groundwater and an insulating layer at the boundary between the flows, which played controlling roles on basement heating and cooling of the overlying lava. It should be stressed that there may be no single, general model to predict the thermal evolution of lava flows.

APPENDIX: LOCATION OF SITES

Subsite FS40, Frenchman Coulee. (47°1'49"N and 119°57'41"W.) A roadcut along old Highway 10 in the south wall of the north alcove of Frenchman Coulee; just east of a spiracle in Roza (Figure 5*b* of *Mackin* [1961]). Evergreen Ridge quadrangle (1:24000): SE 1/4 of SE 1/4, section 20; T18N, R23E.

Subsite FS42, Frenchman Coulee. (47°1'30"N and 119°58'4"W.) At the base of a large pinnacle (Roza); 0.7 km west of site FS40, along old Highway 10. Evergreen Ridge quadrangle (1:24000): SW 1/4 of NE 1/4, section 29; T18N, R23E.

Site DC2, Pasco Basin. (46°34'N and 119°3'W.) Drill hole DC2 at Hanford site; depth 411-420 m below surface. Priest Rapids quadrangle (1:100000): SW 1/4 of NE 1/4, section 35; T13N, R26E.

Site DC12, Pasco Basin. (46°28'N and 119°33'W.) Drill hole DC12 at Hanford site; depth 463-473 m below surface. Richland quadrangle (1:100000): SE 1/4 of NW 1/4, section 3, T11N, R26E.

Acknowledgments. Comments by the late Professor Allan Cox at the 1984 Fall AGU Meeting in San Francisco prompted this study. We thank P. E. Long for advice, discussions, and assistance in obtaining permission to sample the Pasco Basin drill cores, P. E. Long and D. Landon of Rockwell Hanford Operations for help in sampling the drill cores, R. B. Bentley for discussions and showing us Roza outcrops, and G. Bodvarsson for advice in thermal modelling. D. L. Schultz provided invaluable assistance while sampling and in the laboratory. This research was supported by NORCUS and NSF grants EAR 8314211 and EAR 8410376. Reviews by P. Shive, K. Furlong, and K. A. Hoffman contributed to improving the

REFERENCES

Audunsson, H., and S. Levi, A partial geomagnetic transition recorded in a thick Miocene lava flow (abstract), *Eos Trans. AGU*, *65*, 870, 1984.

Beeson, M. H., K. R. Fecht, S. P. Reidel, and T. L. Tolan, Regional correlations within the Frenchman Springs Member of the Columbia River Basalt Group: New insights into the middle Miocene tectonics of northwestern Oregon, *Oreg. Geol.*, *47*, 87–96, 1985.

Bingham, J. W., and K. L. Walters, Stratigraphy of the upper part of the Yakima Basalt in Whitman and eastern Franklin counties, Washington, *U.S. Geol. Surv. Prof. Pap.*, *525-C*, C87–C90, 1965.

Bonacina, C., G. Comini, A. Fasano, and M. Primicerio, Numerical solution of phase-change problems, *Int. J. Heat Mass Transfer*, *16*, 1825–1832, 1973.

Briden, J. C., Ancient secondary magnetizations in rocks, *J. Geophys. Res.*, *70*, 5205–5221, 1965.

Carslaw, H. S., and J. C. Jaeger, *Conduction of Heat in Solids*, 2nd ed., 496 pp., Oxford University Press, New York, 1959.

Clausing, A. M., Numerical methods in heat transfer, in *Advanced Heat Transfer*, edited by B. T. Chao, pp. 156–216, University of Illinois Press, Chicago, 1969.

Cullity, B. D., *Introduction to Magnetic Materials*, 666 pp., Addison-Wesley, Reading, Pa., 1972.

Fuller, R. E., The aqueous chilling of basaltic lava on the Columbia River Plateau, *Am. J. Sci.*, *21*, 281–300, 1931.

Furlong, K. P., and P. N. Shive, Determination of timing of volcanic events by secular variation and thermal modeling, *Geophys. Res. Lett.*, *10*, 701–704, 1983.

Hodges, C. A., Basaltic ring structures of the Columbia Plateau, *Geol. Soc. Am. Bull.*, *89*, 1281–1289, 1978.

Jaeger, J. C., Cooling and solidification of igneous rocks, in *Basalts, The Poldervaart Treatise on Rocks of Basaltic Composition*, vol. 2, edited by H. H. Hess and A. Poldervaart, pp. 503–536, Interscience, New York, 1967.

Levi, S., and R. T. Merrill, A comparison of ARM and TRM in magnetite, *Earth Planet. Sci. Lett.*, *32*, 171–184, 1976.

Levi, S., and R. T. Merrill, Properties of single-domain, pseudo-single-domain, and multidomain magnetite, *J. Geophys. Res.*, *83*, 309–323, 1978.

Long, P. E., and B. Wood, Structures, textures, and cooling histories of Columbia River basalt flows, *Geol. Soc. Am. Bull.*, *97*, 1144–1155, 1986.

Mackin, J. H., A stratigraphic section in the Yakima Basalt and Ellensburg Formation in south-central Washington, *Wash. Div. Mines Geol. Rep. Invest.*, *19*, 45 pp., 1961.

Moak, D. J., Summary of borehole locations and geologic activities at borehole sites, Surface Geology of the Cold Creek Syncline, Appendix A, *Publ. RHO-BWI-ST-14*, Rockwell Hanford Oper., Richland, Wash., 1981.

Murase, T., and A. R. McBirney, Properties of some common igneous rocks and their melts at high temperatures, *Geol. Soc. Am. Bull.*, *84*, 3563–3592, 1973.

Myers, C. W., Yakima basalt flows near Vantage, and from core holes in the Pasco Basin, Washington, Ph.D. thesis, 119 pp., Univ. of Calif., Santa Cruz, 1973.

Néel, L., Théorie du traînage magnétique des ferromagnétiques en grains fins avec applications aux terres cuites, *Ann. Geophys.*, *5*, 99–136, 1949.

Nyblade, A. P., P. N. Shive, and K. P. Furlong, Rapid secular variation recorded in thick Eocene flows from the Absaroka Mountains of northwest Wyoming, *Earth Planet. Sci. Lett.*, *81*, 419–424, 1987.

Packer, D. R., and M. H. Petty, Magnetostratigraphy of the Grande Ronde Basalt, Pasco Basin, Washington, *Publ. RHO-BWI-C-46*, Rockwell Hanford Oper., Richland, Wash., Jan. 1979.

Peck, D. L., M. S. Hamilton, and H. R. Shaw, Numerical analysis of lava lake cooling models, II, Application to Alae Lava Lake, Hawaii, *Am. J. Sci.*, *277*, 415–437, 1977.

Reidel, S. P., and K. R. Fecht, Wanapum and Saddle Mountains Basalts of the Cold Creek Syncline area, Surface Geology of the Cold Creek Syncline, *Publ. RHO-BWI-ST-14*, chapt. 3, pp. 1–45, Rockwell Hanford Oper., Richland, Wash., 1981.

Rietman, J. D., Remanent magnetization of the late Yakima Basalt, Washington State, Ph.D. thesis, 87 pp., Stanford Univ., Stanford, Calif., 1966.

Robertson, E. C., and D. L. Peck, Thermal conductivity of vesicular basalt from Hawaii, *J. Geophys. Res.*, *79*, 4875–4888, 1974.

Shaw, H. R., and D. A. Swanson, Eruption and flow rates of flood basalts, in *Proceedings of the Second Columbia River Basalt Symposium*, edited by E. H. Gilmour and D. Stradling, pp. 271–299, Eastern Washington State College, Cheney, 1970.

Swanson, D. A., T. L. Wright, and R. T. Helz, Linear vent systems and estimated rates of magma production and eruption for the Yakima Basalt on the Columbia Plateau, *Am. J. Sci.*, *275*, 877–905, 1975.

Swanson, D. A., T. L. Wright, P. R. Hooper, and R. D. Bentley, Revisions in stratigraphic nomenclature of the Columbia River Basalt Group, *Geol. Surv. Bull.*, *1457-G*, G1–G57, 1979.

Udell, K. S., Heat transfer in porous media heated from above with evaporation, condensation, and capillary effects, *J. Heat Transfer*, *105*, 485–492, 1983.

Van Alstine, D. R., and S. L. Gillett, Magnetostratigraphy of the Columbia River Basalt, Pasco Basin and vicinity, Washington, *Publ. RHO-BWI-C-110*, 60 pp., Rockwell Hanford Oper., Richland, Wash., June 1981*a*.

Van Alstine, D. R., and S. L. Gillett, Magnetostratigraphy of the Columbia River Basalt, Pasco Basin and vicinity, Washington, *Publ. SGI-R-81-40*, Rockwell Hanford Oper., Richland, Wash., Sept. 1981*b*.

H. Audunsson and S. Levi, College of Oceanography, Oregon State University, Corvallis, OR 97331.

(Received March 30, 1987;
revised August 25, 1987;
accepted August 28, 1987.)